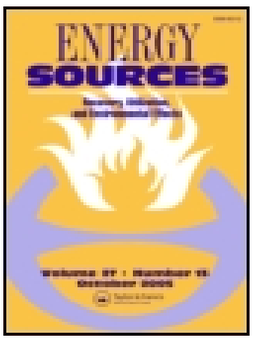

Energy Sources, Part A: Recovery, Utilization, and Environmental Effects

ISSN: 1556-7036 (Print) 1556-7230 (Online) Journal homepage: http://www.tandfonline.com/loi/ueso20

Optimization and characterization of bio-oil produced from cotton shell by flash pyrolysis using artificial neural network

P. Madhu, M. M. Matheswaran & G. Periyanayagi

To cite this article: P. Madhu, M. M. Matheswaran & G. Periyanayagi (2017): Optimization and characterization of bio-oil produced from cotton shell by flash pyrolysis using artificial neural network, Energy Sources, Part A: Recovery, Utilization, and Environmental Effects, DOI: 10.1080/15567036.2017.1403508

To link to this article: http://dx.doi.org/10.1080/15567036.2017.1403508

Published online: 16 Nov 2017.

Submit your article to this journal

View related articles

View Crossmark data

Full Terms & Conditions of access and use can be found at
http://www.tandfonline.com/action/journalInformation?journalCode=ueso20

Download by: [Gothenburg University Library] **Date:** 16 November 2017, At: 23:57

ENERGY SOURCES, PART A: RECOVERY, UTILIZATION, AND ENVIRONMENTAL EFFECTS
https://doi.org/10.1080/15567036.2017.1403508

Taylor & Francis
Taylor & Francis Group

Check for updates

Optimization and characterization of bio-oil produced from cotton shell by flash pyrolysis using artificial neural network

P. Madhu[a], M. M. Matheswaran[a], and G. Periyanayagi[b]

[a]Department of Mechanical Engineering, Jansons Institute of Technology, Coimbatore, Tamilnadu, India; [b]Department of Botany, Raja Doraisingam Government Arts College, Sivaganga, Tamilnadu, India

ABSTRACT

In this work, the effects of pyrolysis parameters such as pyrolysis temperature, feedstock particle size, and sweep gas flow rate on the pyrolysis distributions of cotton shell were tested to identify the optimum bio-oil production conditions. The experiments were conducted in a fluidized-bed reactor with nitrogen atmosphere. The efficient Artificial Neural Network (ANN) was used for modeling and optimizing the process parameters. An ANN model was developed based on the back-propagation learning algorithm to predict the effect of parameters. The experimental data acquired are used for training the network. The results showed that the network yields a maximum bio-oil with minimum coefficient of variance (COV) and root mean square values. The results confirmed that the use of an ANN analysis for pyrolysis distribution is quite suitable. Using the ANN technique, the optimal conditions were found to be at the temperature of 450°C, particle size of 0.8 mm, sweep gas flow rate of 1.75 m^3/h with 52.2 wt% of bio-oil yield. Furthermore, the liquid product was analyzed for physical, elemental, and chemical composition using Fourier transform infrared (FTIR) spectroscopy and gas chromatography (GC).

KEYWORDS

Artificial neural network; bio-oil; cotton shell; pyrolysis; optimization

Downloaded by [Gothenburg University Library] at 23:57 16 November 2017

Introduction

In the rural sectors of India, firewood and charcoal are the two major energy sources for cooking and nonagricultural operations such as pottery, limebrick making, and metal works. The demand for wood is placing an additional strain on forestry areas. Several types of biomass are available from agriculture residues, wood residues, and dedicated energy crops. Among the above-mentioned classifications, agricultural residues have the major potential for developing bio-energy industries (Demirbas, Pehlivan, and Altun 2006). The main advantage of using these residues for energy purposes is that they have a very low market value (Balat 2008). Studies sponsored by the Ministry of New and Renewable Energy have estimated surplus biomass availability at about 150 million metric tons per annum, covering agricultural and forestry residues. Cotton shell has a great potential in this regard, and its composition (hydrogen and carbon) is higher than the other wastes (Madhu, Kanagasabapathy, and Manickam 2016). In India, cotton (*Gossypium arboretum*) crop occupies more than 9.2 million hectares. Cotton wastes are lignocellulosic and can be utilized to produce biofuels. Flash pyrolysis is the process of thermal decomposition of biomass at moderate temperatures in the absence of oxygen to produce liquid, char, and gas (Alper, Tekin, and Karagöz 2015). It is considered as the technology with the greatest potential among other thermochemical conversion processes to produce liquid fuels (Meier and Faix 1999), because it has the benefit of storage and transportation with the potential as a fossil fuel substitute.

CONTACT P. Madhu pnpmadhu@gmail.com Department of Mechanical Engineering, Jansons Institute of Technology, Coimbatore, Tamilnadu 641659, India.

Color versions of one or more of the figures in the article can be found online at www.tandfonline.com/UESO.

© 2017 Taylor & Francis Group, LLC

Theoretical calculations require a large number of geometrical data and assumptions, which are not readily available, whereas experimental calculations are more expensive and time consuming. In most of the earlier pyrolysis reports, the effect of individual parameters on product distributions has been reported while maintaining process parameters as constant. Moreover, interactive effects among the chosen independent variables cannot be showed clearly. These limitations can be eliminated by a statistical experimental design. Response surface methodology (RSM) is believed to be effective for screening key factors rapidly from a multivariable system for optimization (Jo et al. 2008). Besides RSM, ANN technique is a powerful predictive tool for nonlinear multivariate modeling. ANN is a computational technique, which tries to simulate the neurological processing ability of the brain (Archanta et al. 1995). It could be applied for calculating a nonlinear connection between the factors and yield by means of iterative training of the data obtained from a design of experiments. It does not need a prior specification of suitable fitting function and it has universal approximation capability. ANN has the ability of relating the input and output factors without any prior knowledge of the relationship between them.

In this work, the prediction of pyrolysis products is accomplished by ANN. Previously obtained experimental data were used as an input in the ANN study. The output ratios showed variances depending on the pyrolysis temperature, particle size, and sweep gas (N_2) flow rate. The combined effect of the above-mentioned parameters on bio-oil yield has been studied. The ANN model is developed for this purpose via "NNTool" in MATLAB program. The most important aim of this optimization study is to increase the amount of bio-oil. In addition, Fourier transform infrared (FTIR) spectroscopy and gas chromatography (GC) techniques were used to characterize the bio-oil.

Experimental technique

Materials and method

Cotton shells were collected from a local agricultural field from Coimbatore and they were converted into fine particles at different sizes between 0.6 mm and 1.25 mm. The samples were tested, and their results in wt% are volatile matter 62.64, fixed carbon 25.02, moisture content 9.52, ash content 2.82, carbon 45.09, hydrogen 4.90, nitrogen 0.68, oxygen 49.32, and sulfur 0.01. The samples were dried in open sunlight for two weeks to reduce their moisture. Around 600 g of sample was taken for each batch and their feed rate was fixed at 20 g/min. The flow rate of the nitrogen was adjusted to maintain fluidized-bed condition. On pyrolysis, the volatile mater will evolve. After separating the solid particles in a cyclone separator, the condensable volatiles were passed through the condenser to condense as bio-oil. For further analysis, the weight percentages of bio-oil, char, and gas yields were recorded. The experiments were conducted with the reactor, made of stainless steel of 1 m height with 50 mm diameter equipped with nitrogen supply. A 2 kW electric heater was used to heat the reactor and the temperature was recorded by a K-type thermocouple located in five different points inside the reactor. The effect of temperature was investigated first by varying the temperature from 350 to 550°C by keeping the particle size and sweep gas flow rate as constant at 0.71 mm and 1.75 m^3/h, respectively. The next set of experiments was carried out to find the effect of particle size by varying the particle size from 0.6 to 1.25 mm without changing the nitrogen flow rate of 1.75 m^3/h and temperature of 450°C. Finally, the effect of sweep gas flow rate was analyzed by varying the flow rate from 1.25 to 2.4 m^3/h by keeping the particle size as constant at 1 mm and temperature at 450°C.

Artificial neural network

ANN is a mathematical exemplification. It has an input layer and an output layer with one or more hidden layers. The hidden layers are linked to the input and output layers (Achanta et al. 1995). The responses of each neuron in the hidden and output layers are summed and the result is processed by

Downloaded by [Gothenburg University Library] at 23:57 16 November 2017

an activation function (sigmoid function). The method of finding the adjustable weights is known as training the data. Initially the weights are selected randomly and then an iterative algorithm is used to find the weights, which reduces the differences between the actual and calculated outputs (Baughman and Liu 2014). Pairs are selected, fed into the input neurons, and then multiplied by the weights and summed to form net information. The obtained net information is then compressed by the activation function to produce the output.

$$X^{*}=\left\{\frac{(X_{max}-X_{min})}{(X_{max}-X_{min})}*0.8\right\}+0.1 \tag{1}$$

$$X=\left\{\frac{(X_{max}-X_{min})}{0.8}(X*-0.1)\right\}+X_{min} \tag{2}$$

The output obtained at this point was then passed to each neuron in the successive layer and finally the net output was obtained. The obtained outputs were checked with the chosen ones and then the errors were calculated. According to the errors, the generalized delta rule (GDR) was used to adjust the weights. In this study, all the data were randomly separated into two subgroups, such as training and testing (80% and 20% of the data, respectively). To avoid saturation problems, all the data (input and output) were normalized in a uniform range (0.1–0.9). The new scaled values of variables can be found from equation (1), whereas the rescaled values can be obtained from equation (2). Here X^{*} is the scaled value, and X_{max} and X_{min} are the maximum and minimum corresponding variables, respectively. R^2 is the root mean square error (RMSE), and the coefficient of variance (COV) were calculated to evaluate the modeling ability from the equations (3), (4), and (5).

$$R^2=1-\sum_{i=1}^{n}\frac{(y_{ie}-y_{ip})^2}{(y_{ie}-y_{m})^2} \tag{3}$$

$$RMSE=\sqrt{\sum_{i=1}^{n}\frac{(y_{ie}-y_{ip})^2}{n}} \tag{4}$$

$$SEP=\frac{RMSE}{y_{m}}*100 \tag{5}$$

where y_m is the mean experimental bio-oil yield, y_{ie} is the experimental value at point i, y_{ip} is the corresponding predicted yield, and n is the number of experimental data.

Characterization

The bio-oil obtained under the optimized process conditions was used for characterization. Metrohm pH-827 meter was used to evaluate the pH value of the bio-oil. The oil with a measured volume and mass was used to find the density. Viscosity of the bio-oil was measured by the Brookfield LV-DV-II Pro viscometer. The chemical compounds of the oil were determined with THERMO GC-TRACE ULTRA VER: 5.0, THERMO MS DSQ II GC using a 30-m-long DB-35 capillary column (0.25-μm-thick film). The injection port and the detector were set at 250°C. The GC oven was heated to 70°C for 2 min, and then to 250°C at the rate of 10°C/min. An elemental analysis of the sample and bio-oil was carried out by Elementar Vario EL-III. The functional group of the bio-oil was identified by BRUKER Optik GmbH TENSOR 27 FTIR spectroscopy.

Downloaded by [Gothenburg University Library] at 23:57 16 November 2017

Downloaded by [Gothenburg University Library] at 23:57 16 November 2017

Results and discussion

Experimental analysis

The flash pyrolysis experiments were conducted by changing the process parameters such as temperature (350, 400, 450, 500, 550°C), particle size (0.6, 071, 1.0, 1.25 mm), and sweep gas flow rate (1.25, 1.75, 2.0, 2.4 m^3/h). When the temperature was increased from 350 to 450°C, the bio-oil yield increased from 28.95 to 45.28 wt%. The reason for the higher bio-oil yield during this point is the higher decomposition of the condensable volatiles (Islam, Zailani, and Ani 1999). At 350°C, the decomposition rate was low and the char production was high. The same effect was also observed in another study (Gercel 2002). When the temperature was increased from 450 to 550°C, the gas yield is enhanced and the char yield is decreased. Increasing the temperature increases the carbon conversion into gas. By changing the particle size from 0.6 to 1.25 mm, the bio-oil yield will increase from 31.42 to 41.75 wt%. The maximum bio-oil yield of 51.25 wt% was obtained at the particle size of 1.0 mm. When the particle size was increased from 1.0 to 1.25 mm, the distance from the surfaces of the particle to its center is increased, resulting in resistance to heat transfer. Hence, the pyrolysis reaction is incomplete, causing lower bio-oil yield. Based on these outcomes, particle size has a significant effect on yield. The increase in N_2 gas flow rate from 1.25 to 1.75 m^3/h increased the yield of oil from 36.8 to 51.25 wt%. The flow rate of N_2 will affect the residence time of the evolved gases in the hot region, minimizes the secondary decomposition of the higher molecular weight products (Miao, Wu, and Yang 2004). The oil yield is decreased when the N_2 gas flow rate exceeds 1.75 m^3/h due to the fluidization conditions. When the sweep gas flow rate increases, the motion of the particle becomes strong, enhancing the mixing of the fluidized sand material and the biomass. This raises the heat transfer rate, and the release of volatile is increased. During experimentation, the maximum bio-oil yield of 51.25 wt% was obtained at a temperature of 450°C, particle size of 1.0 mm, and at a sweep gas flow rate of 1.75 m^3/h.

Artificial neural network

The ANN structure consists of three neurons in the input layer (reaction temperature, particle size, and sweep gas flow rate), 10 neurons in the hidden layer, and three neurons (bio-oil, char, and gas) in the output layer. The final optimum topology was obtained by finding the number of neurons in the hidden layer iteratively by evolving various networks that differ only with the mass of the hidden layer and instantaneously detecting the change in the mean squared errors (RMSE) (Bas and Boyaci 2007). The structures of the input layers, hidden layers, and output layers form the network topology 3–10–3. Fourteen experimental outcomes were used for training the network. Almost 80% of these data were randomly chosen and trained with the Levenberg–Marquardt algorithm by feed-forward back-propagation. The remaining 20% were used for testing the ANN predictability and model fitness. Table 1 shows the statistical analysis of the ANN. The product distribution is an important parameter that can be considered for proper parameter selection and it can be predicted by ANN; the experimental results are presented in Figure 1. The ANN-predicted values yield a correlation coefficient of 0.9914 for bio-oil production. The RMS and COV values were found to be 0.691 and 1.76 respectively. The ANN-predicted correlation coefficient for char production was 0.9978, whereas the RMS and COV values were found to be 0.285 and 1.20, respectively. For the gas

Table 1. Statistical analysis of ANN.

Particulars	R^2	RMS	COV
Bio-oil	0.9914	0.691	1.76
Char	0.9978	0.285	1.20
Gas	0.9969	0.369	0.99

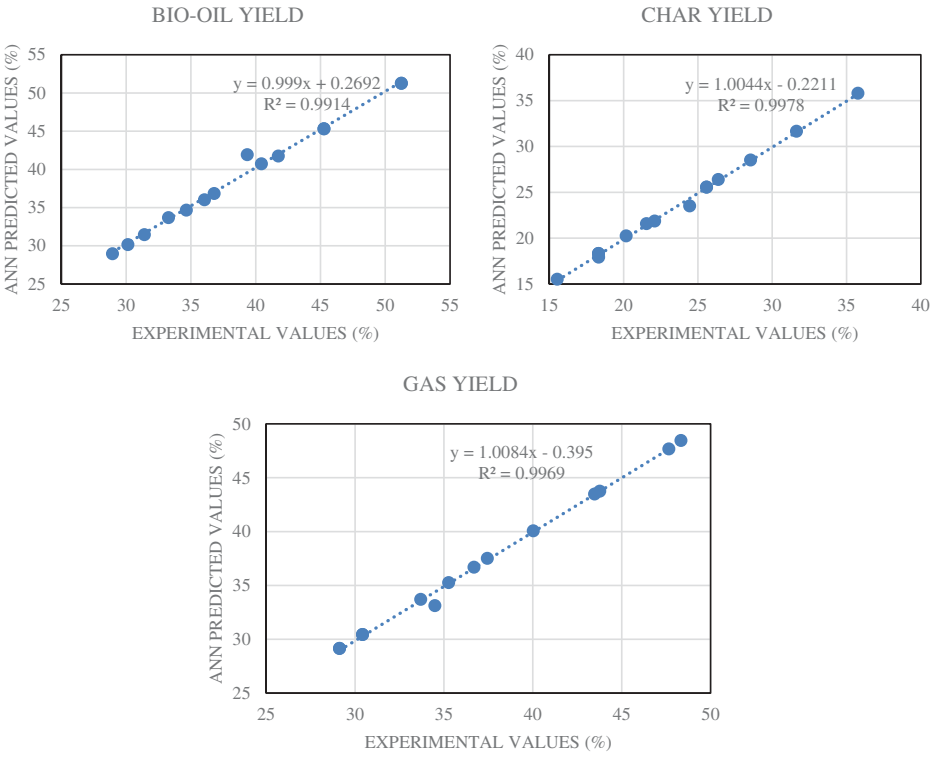

Figure 1. Pyrolysis yield correlation predicted by ANN with the experimental values.

yield, the correlation coefficient was 0.9969, and the RMS and COV values were found to be 0.369 and 0.99, respectively.

The experimental and ANN models were compared and their results were nearly accurate, as shown in Figure 1. This represents the correlation between the experimental and predicted values. The R^2 value for the network topology is almost 1, which elucidates that more than 99% of the response can be explained by the network topology. A comparison of the experimental and ANN-predicted yields is shown in Table 2. The optimum points obtained during the experiment were used for calculating the ANN predictability. The result showed that ANN predicted more bio-oil yield than the experimental value. During experimentation, the maximum bio-oil of 51.25 wt% was obtained at 450°C, 1.0 mm particle size with a sweep gas flow rate of 1.75 m^3/h. However, ANN predicted that the maximum bio-oil yield of 52.2 wt% was obtained with the optimum parameters of temperature 450°C, particle size 0.8 mm, and sweep gas flow rate of 1.75 m^3/h. The higher bio-oil yield at the smaller particle size during ANN prediction suggested that the small particle size can be heated uniformly to evolve more condensable volatiles (Kockar et al. 2000).

Table 2. Optimized parameters for pyrolysis yield using different methodologies.

				Pyrolysis yield in wt%		
Method	Temperature in °C	Particle size in mm	Sweep gas flow rate in m^3/h	Bio-oil	Char	Gas
Experimental	450	1.0	1.75	51.25	18.12	30.43
ANN	450	0.8	1.75	52.20	22.43	25.51

Downloaded by [Gothenburg University Library] at 23:57 16 November 2017

Downloaded by [Gothenburg University Library] at 23:57 16 November 2017

Characterization of the bio-oil product

Physical characterization of bio-oil

Density and viscosity are linked to the ability of the liquid to flow. The density and viscosity of the bio-oil is about 1005 kg/m^3 and 7.87 cSt at 40°C, respectively, and this could be due to the water content (18%) present in the bio-oil. The presence of water is mainly due to the reaction from the lignin content present in the raw biomass. The pH value of the bio-oil is 3.3 at room temperature, which is also reliable. The low pH value can be attributed to the presence of acidic compounds, and it should be traded before being used as a fuel because it can corrode mild steel-, aluminum-, and nickel-based materials. The flash point of the bio-oil is 160 °C. The carbon, hydrogen, nitrogen, sulfur, and oxygen contents of the bio-oil in terms of wt% are 38.14, 11.24, 0.94, 0.11, and 49.57, respectively. The heating value of the bio-oil is found to be 19.32 MJ/kg, which is nearly half of that of gasoline and diesel. The empirical formula of bio-oil is $CH_{3.511}N_{0.0211}O_{0.975}$.

Chemical compositions

The FTIR spectra of bio-oil are shown in Figure 2. The O–H stretching vibrations at 3433.94 cm^{-1} specify the presence of polymeric hydroxyl compounds, phenols, and alcohols. The C = C stretching vibrations at peak 1639.72 cm^{-1} indicate the presence of alkanes and aromatics. The –CH_2 bending at 1407.13 cm^{-1} indicates the presence of alkanes group. The skeletal vibration at 1054.91 cm^{-1} indicates the presence of cyclopropanes and the in-plane ring bending of pyridine (–N–H) appears at 658.28 cm^{-1}. Various types of compounds present in the bio-oil can be identified using GC-MS, as shown in Table 3. The available products with peak areas greater than 10% are 2-methoxyphenol and 2,6-dimethoxyphenol. The oxygenated aromatic (ArO) compounds of phenols, acids, and aldehyde

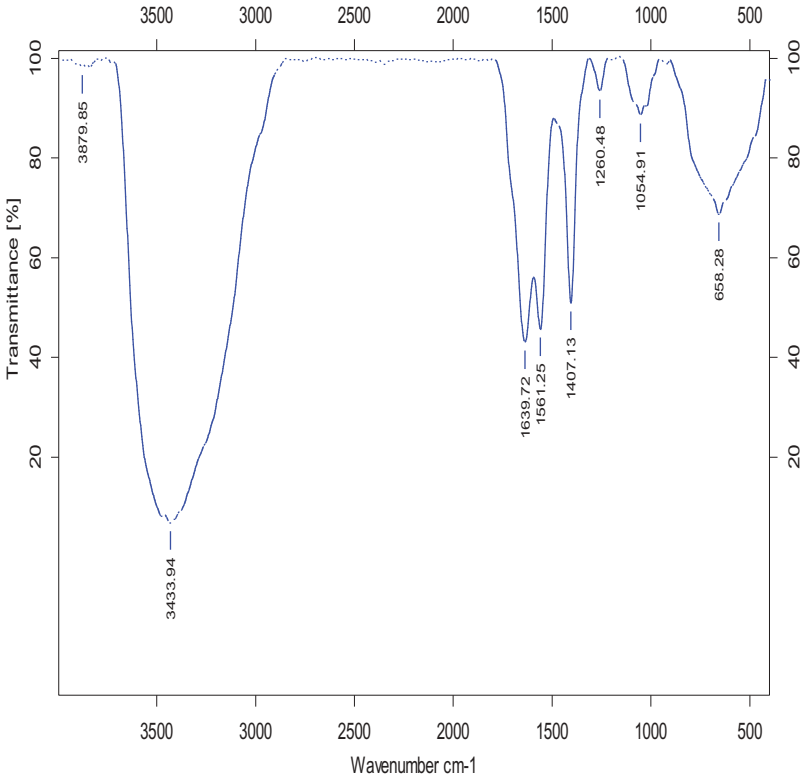

Figure 2. FTIR spectra of the bio-oil.

Downloaded by [Gothenburg University Library] at 23:57 16 November 2017

Table 3. Identification and quantification of chemical compounds in bio-oil by GC-MS analysis.

Chemical compound	Molecular formula	Molecular weight	Type of compound	Structure	% Peak area
3,4-Dimethylthiophene	C_6H_8S	112	NAr	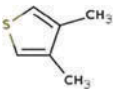	2.22
Phenol, 2-methoxy	$C_7H_8O_2$	124	ArO	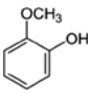	12.93
2-Methoxy-4-methylphenol	$C_8H_{10}O_2$	138	ArO	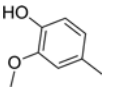	1.93
2,5-Dimethoxytoluene	$C_9H_{12}O_2$	152	ArO	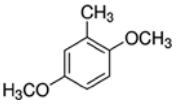	3.07
Phenol, 2,6-dimethoxy	$C_8H_{10}O_3$	154	ArO	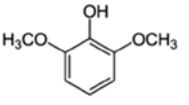	10.42
Tetradecane	$C_{14}H_{30}$	198	NAr		0.35
3-Hydroxy-4-methoxybenzoic acid	$C_8H_8O_4$	168	ArO	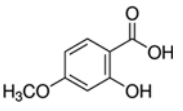	1.61
4,5-Dimethoxy-2-(2-propenyl) phenol	$C_{11}H_{14}O_3$	194	ArO	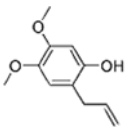	0.48
2-Phenyl-1-p-tolylethanol	$C_{14}H_{16}O$	200	ArO	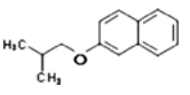	1.88

are the leading compounds. Phenolics are also identified as the main compounds of bio-oil (Capunitan and Capareda 2012). These types of compounds occur profusely since they exist as monomeric units and oligomers from the lignin in the biomass (Ates and Isikdag 2008). Every compound is classified as ArO and nonaromatic (NAr). The thermal degradation of the oxygenated

components of the cotton shell is the main reason for the presence of these compounds in the bio-oil. In general, aldehyde and phenols are the reason for the thermal instability of the bio-oil.

Conclusion

In this study, a rotatable central composite design was carried out to investigate the effects of pyrolysis parameters on pyrolysis distribution. During this study, temperature was found as the most significant parameter in optimization compared to particle size and sweep gas flow rate. ANN predicted the maximum bio-oil yield of about 52.2 wt% at an optimum temperature of 450°C with a particle size of 0.8 mm and a sweep gas flow rate of 1.75 m^3/h. Thus, the neural network model has better predictability in accuracy than the experimental investigation. The bio-oil obtained during the optimum point contains various organic compounds of carbon, which was dominated by ArO. FTIR analysis of the bio-oil sample showed that the bio-oil composition is dominated by oxygenated species.

References

Achanta, A. S., J. G. Kowalski, and C. T. Rhodes. 1995. Artificial neural networks: Implications for pharmaceutical sciences. *Drug Development and Industrial Pharmacy* 21 (1):119–55. doi:10.3109/03639049509048099.

Alper, K., K. Tekin, and S. Karagöz. 2015. Pyrolysis of agricultural residues for bio-oil production. *Clean Technologies and Environmental Policy* 17 (1):211–23.

Ates, F., and M. A. Isikdag. 2008. Evaluation of the role of the pyrolysis temperature in straw biomass samples and characterization of the oils by GC/MS. *Energy Fuels* 22:1936–43.

Balat, M. 2008. Mechanisms of thermochemical biomass conversion processes. Part 1: Reactions of pyrolysis. *Energy Sources, Part A* 30 (7):620–35.

Bas, D., and I. H. Boyaci. 2007. Modeling and optimization II: Comparison of estimation capabilities of response surface methodology with artificial neural networks in a biochemical reaction. *Journal of Food Engineering* 78 (3):846–54.

Baughman, D. R., and Y. A. Liu. 2014. *Neural networks in bioprocessing and chemical engineering*. San Diego, CA: Academic Press.

Capunitan, J. A., and S. C. Capareda. 2012. Assessing the potential for biofuel production of corn stover pyrolysis using a pressurized batch reactor. *Fuel* 95:563–72.

Demirbas, A., E. Pehlivan, and T. Altun. 2006. Potential evolution of Turkish agricultural residues as bio-gas, bio-char and bio-oil sources. *International Journal of Hydrogen Energy* 31 (5):613–20.

Gercel, H. F. 2002. The production and elevation of bio oils from the pyrolysis of sunflower oil cake. *Biomass Bioenergy* 23 (4):54–65.

Islam, M. N., R. Zailani, and F. N. Ani. 1999. Pyrolytic oil from fluidised bed pyrolysis of oil palm shell and its characterisation. *Renewable Energy* 17 (1):73–84.

Jo, J. H., D. S. Lee, D. Park, W. S. Choe, and J. M. Park. 2008. Optimization of key process variables for enhanced hydrogen production by Enterobacter aerogenes using statistical methods. *Bioresource Technology* 99 (6):2061–66.

Kockar, O. M., O. Onay, A. E. Putun, and E. Putun. 2000. Fixed-bed pyrolysis of hazelnut shell: A study on mass transfer limitations on product yields and characterization of the pyrolysis oil. *Energy Sources Part A* 22:913–24.

Madhu, P., H. Kanagasabapathy, and I. N. Manickam. 2016. Cotton shell utilization as a source of biomass energy for bio-oil by flash pyrolysis on electrically heated fluidized bed reactor. *Journal of Material Cycles and Waste Management* 18 (1):146–55.

Meier, D., and O. Faix. 1999. State of the art of applied fast pyrolysis of lignocellulosic materials: A review. *Bioresource Technology* 68 (1):71–77.

Miao, X., Q. Wu, and C. Yang. 2004. Fast pyrolysis of micro algae to produce renewable fuels. *Journal of Analytical and Applied Pyrolysis* 71:855–63.

Downloaded by [Gothenburg University Library] at 23:57 16 November 2017